Summer 8-2018

The Transition from Sevier to Laramide Orogeny Captured in Upper-Plate Magmatic Structures, Eastern Transverse Ranges, CA

Brody Friesenhahn
Southern Methodist University, brodyfriesenhahn@gmail.com

THE TRANSITION FROM SEVIER TO LARAMIDE OROGENY CAPTURED IN UPPER-PLATE SYN-MAGMATIC STRUCTURES, EASTERN TRANSVERSE RANGES, CA

Approved by:

Dr. Rita C. Economos
Assistant Professor of Igneous Petrology

Dr. Robert Gregory
Professor Dept. Chair Geochemistry

Dr. James E. Quick
Associate Vice President for Research
Dean of Graduate Studies
Professor of Earth Sciences

Dr. R. E. Powell
United States Geological Survey

THE TRANSITION FROM SEVIER TO LARAMIDE OROGENY CAPTURED IN UPPER-PLATE SYN-MAGMATIC STRUCTURES, EASTERN TRANSVERSE RANGES, CA

A Thesis Presented to the Graduate Faculty of

Dedman College

Southern Methodist University

in

Partial Fulfillment of the Requirements

For the degree of

Master of Science

With a

Major in Geology

by

Brody Friesenhahn

B.S., Geology, University of Texas at Austin

August 7, 2018

ACKNOWLEDGEMENTS

"A sadder and wiser man he rose the 'morrow morn"

- Samuel Taylor Coleridge

Friesenhahn, Brody B.S., Geology, University of Texas at Austin

<u>The Transition from the Sevier to Laramide Orogeny Captured in Upper-Plate Syn-Magmatic Structures, Eastern Transverse Ranges, CA</u>

Advisor: Professor Rita Economos

Master of Science conferred August 7, 2018

Dissertation completed August 7, 2018

The onset of the Laramide orogeny is of great tectonic significance to the geologic history of the US, but the timing and nature of the shift between Sevier and Laramide tectonics remains enigmatic. The eastern Transverse Ranges of southern California provide the opportunity to observe the effects of Laramide tectonics on the mid-crust. Wide Canyon is a north/south-trending canyon in the northern Little San Bernardino Mountains of the eastern Transverse Ranges. Al-in-hornblende thermobarometry of Needy *et al.* (2009) yields a projected paleodepth depth of ~20 km for Wide Canyon where Cretaceous granitoids intrude metamorphic country rock of Proterozoic age in a regional NW-trending antiform.

U/Pb geochronology of five igneous samples from Wide Canyon reveals two zircon growth events at 88-84 Ma (32 analyses) and 76-72 Ma (30 analyses). Granite, granodiorite and gabbro samples contain zircons with 88-84 Ma cores and 76-72 Ma rims. One granite sample yielded a unimodal age of 74.1 ± 1.6 Ma. U and Th concentrations among 88-84 Ma zircon cores span three and four orders of magnitude in concentration, respectively, as would be expected from samples that range from granite to gabbro. In contrast, 76-72 Ma zircon rims yield U-Th concentrations that are within an order of magnitude.

Syndeformational structures such as a regional synmagmatic shear zone, melt-filled parasitic folds and a melt-filled field area-scale antiform are constrained by the reported 76-72

Ma zircon ages. Shear sense indicators in the southwest-dipping shear zone (S/C fabrics, sigma and delta clasts and asymmetric boudins) yield strong top-to-the-northeast kinematics.

The bimodal age distributions coincide with the shift from Sevier to Laramide tectonics during the Late Cretaceous. 88-84 Ma zircon ages are interpreted as a pulse of arc-magmatism during the Sevier Orogeny. Mafic rocks of synchronous age found in the arc-derived Teutonia batholith bear compositional similarities to mafic rocks of Wide Canyon, indicative of similar magmatic sources from 88-84 Ma.

Zircon ages of 76-72 Ma zircon ages are interpreted as recording a shearing event, the emplacement of some granite bodies, and widespread zircon overgrowth. Top-to-the-northeast kinematics in the southwest-dipping synmagmatic regional shear zone are interpreted as backthrusting during northwest/southeast regional contraction that is well constrained by U/Pb zircon geochronology. This contraction is interpreted as the onset of Laramide tectonics between 76-72 Ma. The timing for the onset of flat slab subduction in the Mojave section of the Cordilleran arc is much later than is presumed by proposed tectonic models.

TABLE OF CONTENTS

LIST OF FIGURES

CHAPTER 1

INTRODUCTION

Subduction of the oceanic Farallon plate beneath the continental North American plate during the early Late Jurassic yielded an abundance of arc-derived igneous rocks emplaced into thick, heated continental crust along the Cordilleran Arc (e.g., DeCelles, 2004). During the Late Cretaceous, a shift occurred between tectonic regimes, as the more archetypical style subduction of the Sevier Orogeny gave way to the 500-km-wide band of thick-skinned deformation of the Laramide Orogeny (Dickinson and Snyder, 1978). Based on the observation that magmatism swept eastward, shallow slab subduction is thought to have migrated inland during the late Cretaceous, leading to the cessation of traditional arc magmatism along the Cordilleran Arc by approximately 85 Ma (Coney and Reynolds, 1977; Saleeby 2003, Liu, *et al.,* 2010).

Flat slab subduction in the Cordilleran Arc is attributed to the subduction of the conjugates of the aseismic Hess and Shatsky Rise (Saleeby, 2003; Wells and Hoisch*,* 2008; Liu *et al.,* 2010; Copeland *et al.,* 2017). It is inferred that the Mojave segment of the Cordilleran arc experienced alternating periods of shortening and extension in response to the Laramide Orogeny during the shearing away of the mantle wedge and upper crust, the ensuing underplating of Franciscan derived sediments, and the subsequent destabilization of Laramide orogenic structures (Humphreys, 1995; Saleeby, 2003 Wells and Hoisch, 2008). Crustal shearing and underplating of accretionary wedge sediments occurred at approximately 9 kb leading to deformation and fluid flux into the mid-crust (Sharry, 1981; Pickett and Saleeby, 1993; Jacobson, 1995).

Copeland *et al.,* (2017) assign an approximate age of 90 Ma to the initiation of Laramide-related surface uplift along the Cordilleran arc as the Farallon plate migrated to the northeast beneath the North American plate based on a compilation of magmatic ages paired with field observations. Reconstructions based on seismic velocities beneath North America and the positions of the conjugate rises relative to the current Pacific spreading center place the edge of the subducting Farallon plate and related magmatism more than 1000 km inland of the trench of the Cretaceous Cordilleran Arc (Liu *et al,* 2010). The Mojave section of the Cretaceous Cordilleran Arc is a poor fit to such models, as Late Cretaceous magmatism remained persistent across portions of southern California long after the estimated onset of Laramide flat-slab subduction (Fig. 1; Calzia *et al*., 1986; Barth *et al*., 2004; Needy *et al*., 2010).

An abundance of Late Cretaceous mid- to upper-crustal igneous rocks, which intruded Triassic and Jurassic arc rocks and Proterozoic metamorphic country rock, compose the Mojave section of the Cretaceous Cordillera (Powell, 1981; Barth *et al.,* 2009; Needy *et al.,* 2009). Al in hornblende thermobaramotry across the eastern Transverse Ranges revealed a east-dipping tilted crustal section, preserving ~6 km paleodepths in the east near the 1700 km^2 Cadiz Valley batholith (Anderson, 1988), to approximately 19 km paleodepths in the west prior to the truncation of the tilted crustal section at the San Andreas Fault (Needy *et al.,* 2009). The field area that is the subject for this study, Wide Canyon, is a north/south trending 16-km-long canyon that transects the deepest portion of the tilted crustal section in the northern Little San Bernardino Mountains. The geology of Wide Canyon preserves structures and magmatism that cross the temporal transition from Sevier to Laramide orogenesis.

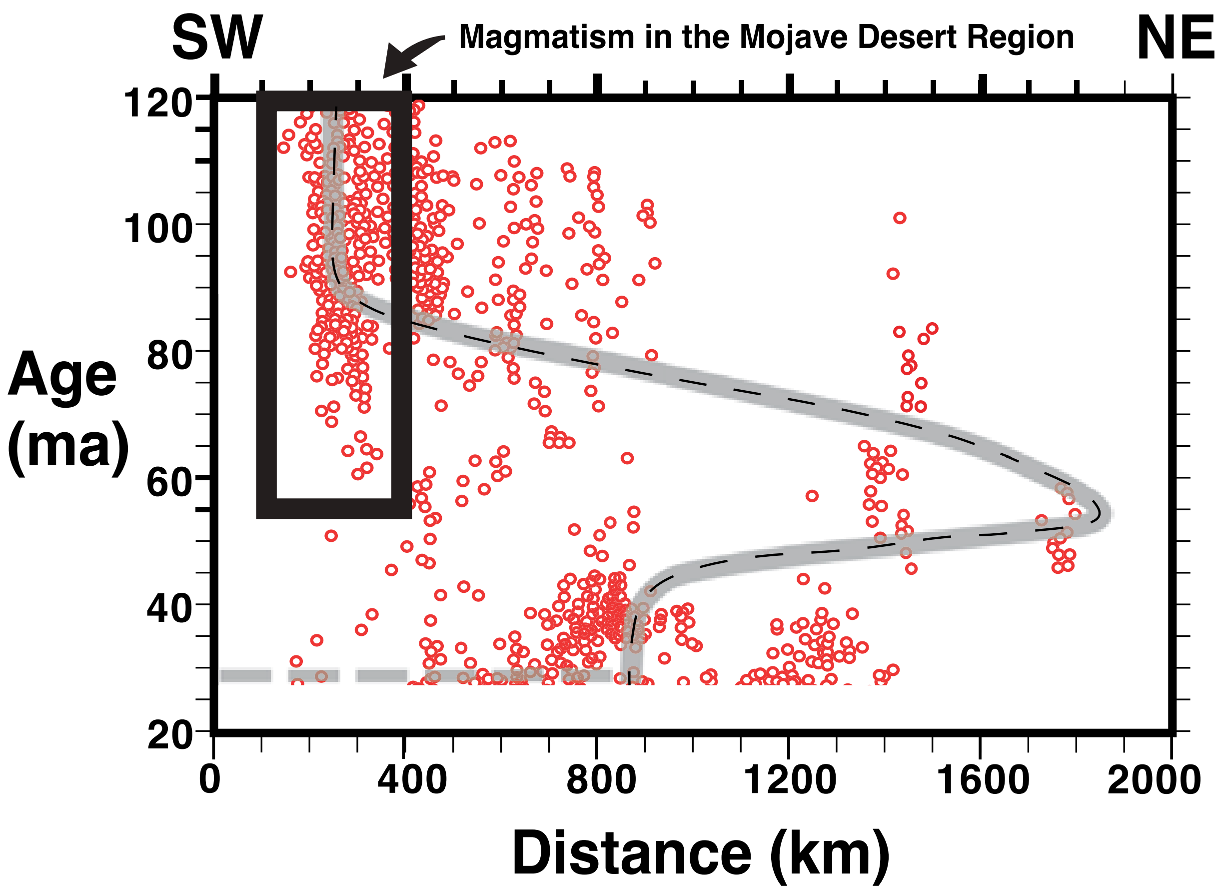

Figure 1. Magmatism of the Laramide Orogeny. Red circles indicate the distribution of magmatic rocks between 120 and 20 Ma. The boldened rectangle indicates the location of the Mojave Desert Region. Gray line represents the leading edge of the Farallon Plate. NE/SW trend of projected data begins off the southern California coast and ends in the southwest corner of North Dakota. Modified from Copeland *et al.,* 2017 (Coney and Reynolds, 1977).

Through geologic mapping and U-Pb in zircon geochronology, this study explores the nature of shifting tectonic regimes across the Mojave section of the Cretaceous Cordillera by placing constraints on the timing of magmatism and its relationship to crustal structures. Shifting source materials are also elucidated by whole rock and zircon geochemistry. These observations reveal two distinct periods of zircon growth and magma emplacement into the mid crust during the late Cretaceous. Arc-derived magmas were emplaced at 88-84 Ma in extensive sill like intrusions during the Sevier Orogeny with preserved igneous rock compositions predominantly controlled by the pre-existing country rock variability. Mid-crustal synkinematic magma emplacement and widespread zircon overgrowth of relatively homogeneous trace element and isotopic composition occurred from 76-72 Ma. Paleo-NE-SW shortening with a top-to-the-northeast sense of shear is elucidated by the orientations of a synmagmatic shear zone, a regional antiform and abundant parasitic fold axes. These structures are interpreted as a primary back-thrust of the Laramide contractional system.

CHAPTER 2

GEOLOGIC SETTING

The study area is in the east-west trending eastern Transverse Ranges of the western Mojave Desert region of southern California, which are composed of Proterozoic basement rocks, Mesozoic plutons of various ages and compositions, and Mesozoic volcanic and sedimentary rocks, spanning Cretaceous age ranges from 90 Ma to 72 Ma (Powell, 1981, 1993; Tosdal *et al.,* 1989; Barth and Wooden, 2006; Needy *et al.,* 2009; Barth *et al.,* 2009). Proterozoic basement in the eastern Transverse Ranges includes both metaigneous and metasedimentary rocks of approximately 1.7 Ga, which, at approximately 1.4 Ga, were intruded by a series of granitoid plutons (Anderson and Bender, 1989; Anderson and Morrison, 1992; Barth *et al*., 2001).

The onset of the Laramide Orogeny resulted in the differential exhumation of the eastern Transverse Ranges yielding exposures of deep crustal rocks in the western portion of the Mojave Desert and shallow crustal rocks in the east (Anderson, 1988; Barth and May 1992). Al-in-hornblende thermobarometry yields solidus pressures from 2 to 6 kb, revealing an approximately 8° east-dipping tilted crustal section (Schmidt, 1992; Needy *et al.,* 2009). Voluminous shallow crustal batholiths to the east (Cadiz Valley and Teutonia batholiths) are underlain by intermediate plutons, and thin sill-like intrusions of a mid-crustal sheeted magmatic complex now exposed to the west. These deeper-seated rocks were emplaced at approximately 20 km paleodepth (Barth *et al*., 2009; Needy *et al.,* 2009) uplifted, and then truncated by the San Andreas Fault.

The study area preserves compositionally and geochemically diverse Mesozoic plutonic rocks. Intrusive units are typically medium to high potassium, calc-alkaline, silicic (>66%) granitoids that exhibit mineralogic compositions between two-mica granites and hornblende-biotite granodiorite (Barth *et al.,* 2009). Radiogenic isotopic analyses across the field area reveal more evolved isotopic signatures than surrounding regions such as the Sierra Nevada Batholith (DePaolo, 1981; Kistler and Ross, 1990). $^{87}Sr/^{86}Sr_{(t)}$ values range from 0.707 to approximately 0.714; this evolved isotopic character matches well with the older ages of the bulk continental crust in this region. Whole rock δ18O values range from 7-9 per mil, identical to the range recorded in the western Sierra Nevada Batholith and the Peninsular Ranges Batholith (e.g., Lackey *et al.,* 2008), suggesting some consistency in magmatic processes between the systems. (Barth *et al.*, 2008; Solomon *et al.,* 1989**;** Barth *et al.,* 1992**;** Barth *et al.,* 1995**;** Mayo *et al.,* 1998; Weigand *et al.,* 2007).

The uppermost portions of the tilted crustal section host the Cadiz Valley Batholith (CVB). The CVB is an extensive 1700 km^2 composite body of granite-dominated rocks spanning from the Coxcomb/Sheep Hole Mountains to the Iron Mountains (Howard and John, 1984; Calzia, 1982; Howard, 2002; Barth *et al.,* 2004). The CVB intrudes gneissic country rock of Proterozoic age, Jurassic igneous rocks at its western margin and the metasedimentary, Jurassic to Cretaceous McCoy Mountains Formation at its southern margin. U-Pb zircon geochronology of porphyritic biotite granite from the CVB yields ages of 73.9 ± 1.3 Ma. Other large Cretaceous plutonic bodies include the Teutonia Batholith. Lying approximately 100 km north of the CVB, the Teutonia Batholith is a composite, granodiorite-dominated body covering 300 km^2 with U-Pb zircon ages from 88-82 Ma (Barth *et al.,* 2004).

Intermediate plutons of Triassic, Jurassic and late Cretaceous ages are abundant across the eastern Transverse Ranges (Needy *et al.,* 2009). The Late Cretaceous intermediate plutons are closely related to the synchronous construction of the underlying sheeted complex (Needy *et al.,* 2009; Ianno, 2008). This northwest trending sequence of parallel-layered m to decimeter thick intrusive units disrupts surrounding Proterozoic gneissic country rock. This unit is exposed from depths of approximately 13-17 km and present at the upper portions of Wide Canyon (Needy *et al.,* 2009).

The Little San Bernardino Mountains are situated in the westernmost eastern Transverse Ranges, in close proximity to the San Andreas Fault, and are composed of mostly Cretaceous plutons of granitoid composition intruding gneissic and metasedimentary and metaigneous host rock of Proterozoic ages. Due to the clockwise rotation of the eastern Transverse Ranges along the San Andreas Fault, the region is characterized by abundant sinistral east-striking faults (Powell, 1981, 1993; Carter *et al.,* 1987; Langenheim and Powell, 2009).

Needy *et al.* (2009) indicate that the deepest projected paleodepths of the crustal section in the Little San Bernardino Mountains are approximately ~20 km (Needy *et al.,* 2009). Such depths are analogous to the depths of the bottom of the modern-day low velocity zone of the Altiplano Puna Magma Body of the Central Volcanic Zone of the Andes (Ward *et al.,* 2014), but are less than the depths suggested for the original emplacement of forearc schists of the Pelona-Orocopia-Rand suite that are ultimately juxtaposed against Cretaceous plutonic rocks, cutting out significant portions of lower crust. These deep exposures therefore are the most likely place to glean insights into the evolution of this dramatic tectonic event.

CHAPTER 3

ANALYTICAL METHODS

Mapping

Geologic mapping was completed at a 1:10,000 scale using digital topographic base maps from the USGS (https://viewer.nationalmap.gov/). 800 m of relief and rugged topography limited mapping to the immediate area of Wide Canyon. Goals of mapping were to identify plutonic features, to characterize their internal structures and relationships with Proterozoic host rocks and relative dating of plutonic rocks, host rocks and deformation events.

Fieldwork resulted in the generation of a new geologic map of Wide Canyon within the Little San Bernardino Mountains, of the eastern Transverse Ranges. Digital map generation was completed in ArcGIS®, QGIS and Adobe Illustrator®. All geologic map elements (font, text size, unit/element colors, contacts, and structural data) were selected in accordance to specific USGS guidelines. All geochemical and structural data will be stored in an open geodatabase upon publication.

Geochronology

8 samples of both metamorphosed and unmetamorhposed syenogranite to granodiorite and gabbro were analyzed for U/Pb in zircon geochronology via SHRIMP-RG at Stanford University. Sub-sample aliquots were crushed and ground by rock crusher and disk mill to a modal grain size of 250 μm. Ground sample were then sieved to 250-50 μm. By panning, heavy minerals were separated prior to density separation using lithium metatungstate (LMT). Zircons were hand picked using a stereoscope. To minimize the effects of Pb loss in zircon rims, all

grains were subject to thermal annealing. Individually picked grains were transferred to quartz glass dishes via pipette. Grains were dried and exposed to temperatures of 900 °C for 48 hours. Zircon grains were removed from quartz glass dishes via pipette and mounted on one inch round epoxy pucks. Surfaces were exposed via polishing with 1200 grit paper and 3 and 1 micron diamond suspension and subsequently imaged using cathodoluminescence (CL) microscopy and analyzed by SHRIMP-RG.

Upon SHRIMP-RG analysis, primary O^- beam creates a spot of approximately 20 μm from which secondary ions were extracted. Ion counters (electron multipliers) were utilized to collect all species, reported in counts per second. Typical calibration methods were used to calculate U/Pb fractionation factors using Braintree R33-TE and trace element concentrations were calculated using 91500 as a standard **(**Black *et al.,* 2004; Wiedenback 2004**).** The high transmission at high mass resolution (~4500) of the SHRIMP-RG allows for the collection of U-Pb geochronology and trace element concentrations in a single magnet pass, meaning from the same analytical aliquot.

CHAPTER 4

RESULTS

Mapping

Wide Canyon preserves a NW-trending broadly antiformal section of the Little San Bernardino Mountains with Proterozoic metaigneous and metasedimentary country rocks intruded by Cretaceous granitoids and gabbros (Fig. 2). Geologic units of Wide Canyon can be divided into three main assemblages; the Magmatic Sheeted Complex, Middle Wide Canyon and Lower Wide Canyon.

Assemblages and Structures of Wide Canyon

The Magmatic Sheeted complex (Barth and Wooden, 2010): comprised of north-dipping structurally coherent m scale sill-like intrusions of Cretaceous granitoids into Proterozoic country rock. Igneous intrusions include foliated inequigranular granite, granodiorite and gabbroic sills oriented parallel to country rock foliations (Fig. 3a). Igneous foliations of the same orientation are common among sheeted magmatic complex units, typically defined by meter-scale intrusions of compositionally variable granitoids. With increasing magma abundances down canyon, the sheeted complex begins to lose structural coherency giving way to a zone of sheared igneous rocks. The Sheeted Complex Assemblage of Upper Wide Canyon yields both hyper and subsolidus foliations from 220-300° (Fig. 4)**.** Upper Wide Canyon bears an abundance of subsolidus foliations based upon the absence of undeformed quartz and plagioclase crystals. With increasing depth in the canyon, hypersolidus foliations become more abundant.

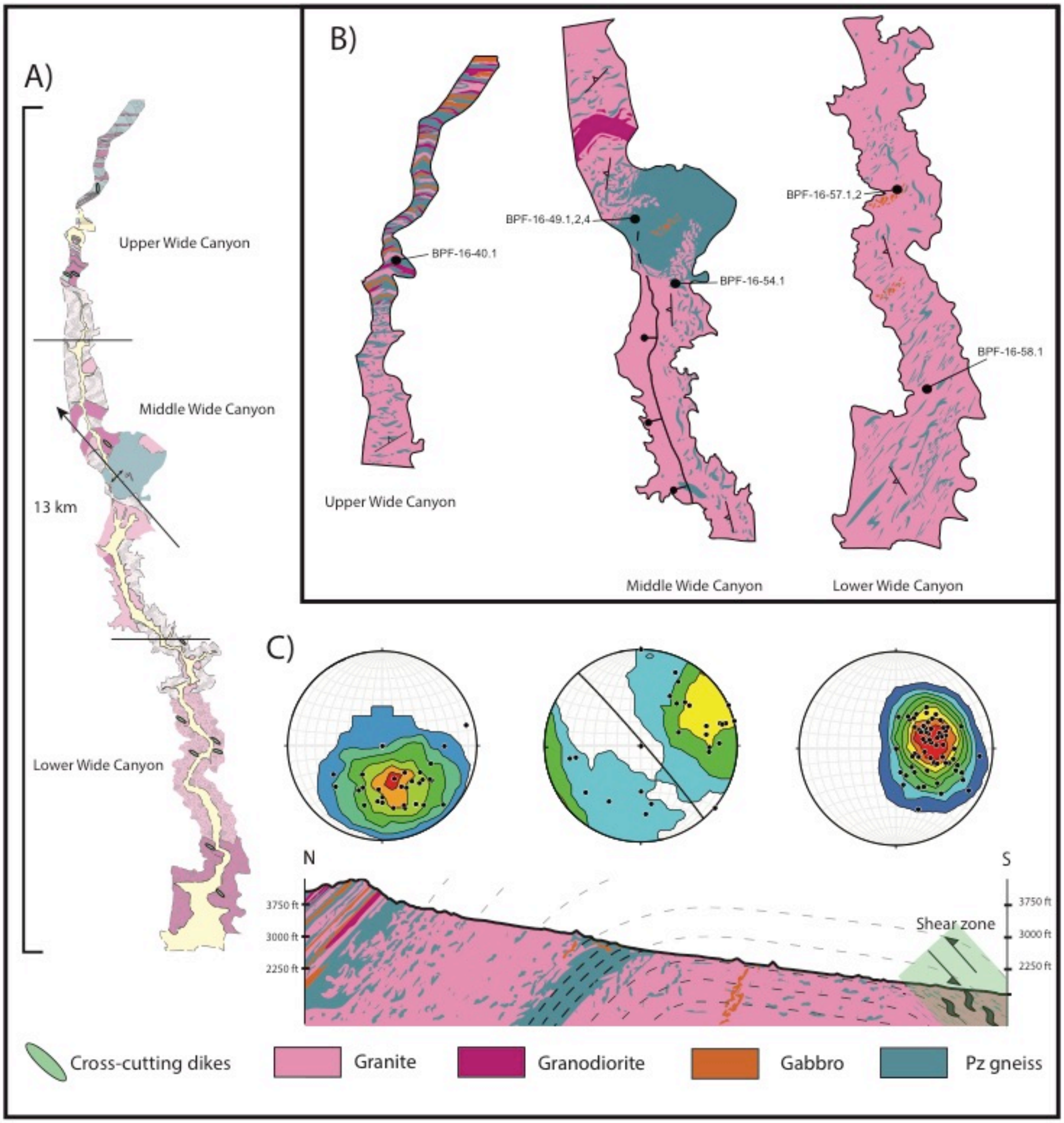

Figure 2. Simplified geologic map of Wide Canyon. A broad northeast trending antiform reveals mid crustal exposures of Proterozoic country rock intruded by Cretaceous granitoids. Lower Wide Canyon bears highly sheared granitoids in a km scale melt-dominated migmatite unit. U/Pb geochronology sample localities are noted by black dots.

Middle Wide Canyon Assemblage: Garnet bearing paragneissic unit of Proterozoic age lies in the core of a regional antiform (Fig. 3b). Almandine porhyroblasts, ranging from 0.5 to 1 cm in diameter, form coherent garnet clusters in pristine cm scale biotite/amphibole melanosomes. In outcrop, deformed quartz/plagioclase ribbons define subsolidus foliations from 180 to 230°. This unit preserves strong evidence of synmagamtic deformation in the form of an abundance of melt filled parasitic folds of heterogeneous thickness. Synmagmatic folds of Middle Wide Canyon yield an average axial plane trend of 319°, indicating a northeast/southwest σ_1 direction at the time of magma emplacement. (Fig. 4).

A north/south trending normal fault in the center of Wide Canyon is west dipping between 45 and 65°. This young normal fault places Proterozoic aged paragneiss and migmatites in the footwall and sheared granites in the hanging wall. Shearing in granites occurred at hypersolidus conditions and is not the result of this faulting, which, based on the presence of a gouge zone, is interpreted as being a much younger low temperature feature. Smaller faults and joints are present in the same orientation as large-scale canyon-forming faults striking 300°, such faults are often times filled with late stage aplite dikes (trending 300°).

Lower Wide Canyon Assemblage: A 3 km continuous exposure of a synmagmatic shear zone is defined by strongly sheared migmatite units. Foliated granitoids and schollen/schlieren structure diatexite migmatites with highly deformed paleosome rafts, residuum and gabbroic enlcaves suspended in a strongly foliated granitoid matrix (Fig. 3c). Granitoid matrices are highly diverse among the laterally extensive assemblage, with an array of compositions, textures, and fabrics. Compositions are often times variable on the basis of hornblende abundance near mafic country rock units.

Lower Wide Canyon is dominated by strong hypersolidus foliations striking 130° to 170° in the southern limb of the regional antiform (Fig. 4)**.** Lineations plunge approximately 20° toward 200 and 245°. Abundant kinematic indicators yield a strong top to the northeast sense of shear. While sigma and delta clasts of biotite and hornblende are the most common indicators in outcrop, asymmetric boudins and S and C fabrics are present and also indicate top the northeast shear sense (Fig. 4). Observed sense of shear is indicative of thrust orientation, constraining the antiformal structure of Wide Canyon to the thrust's footwall.


B)

Figure 3. Wide Canyon Assemblages. A) Sheeted Complex of Upper Wide Canyon. B) disrupted Proterozoic gneiss of Middle Wide Canyon. Disrupted rocks include gneissic schollen and restitic blocks. C) Regional shear zone of Lower Wide Canyon.

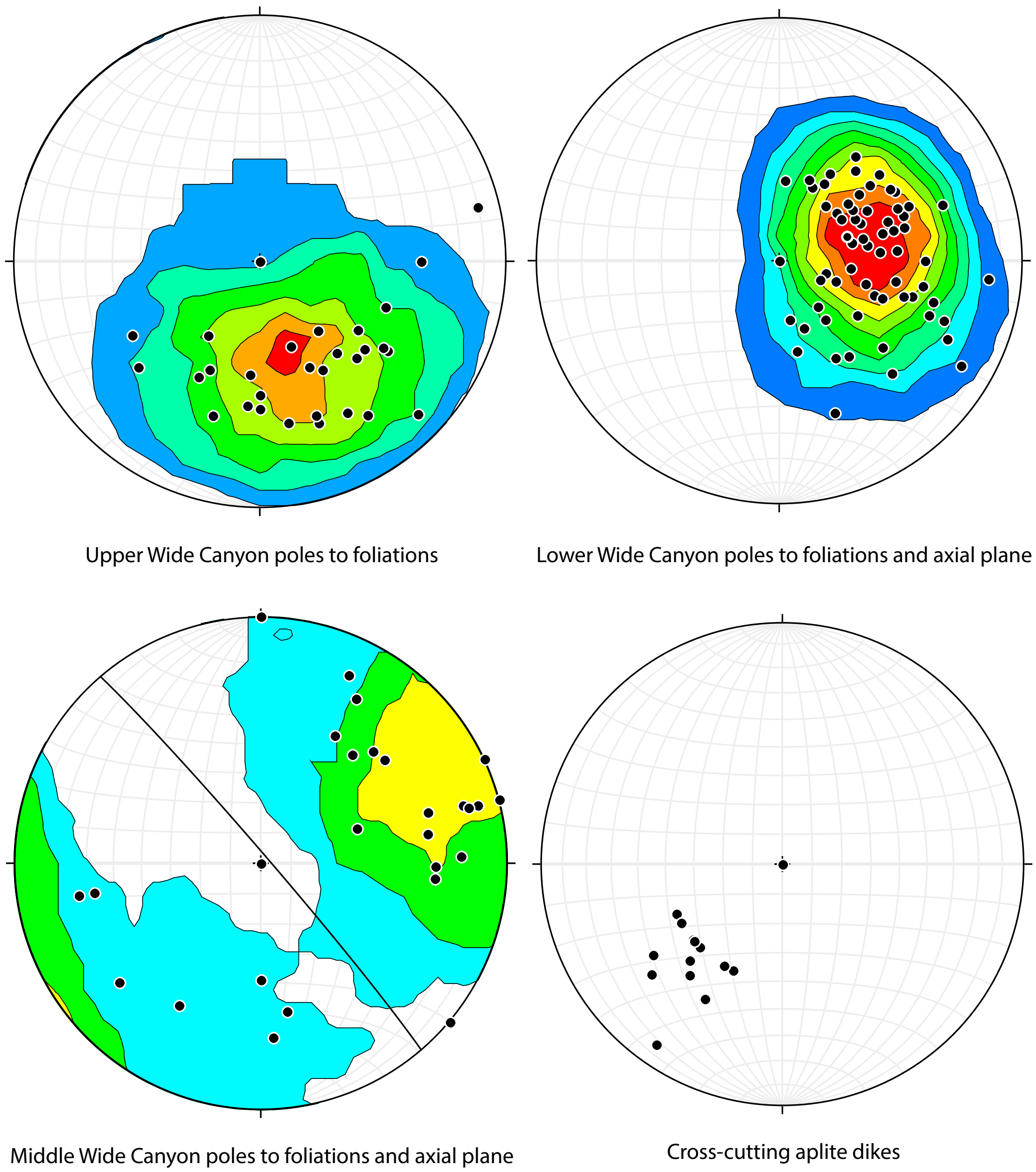

Figure 4. Structural measurements of Wide Canyon. A) Magmatic foliations of Upper Wide Canyon (3769000-3765000 N). B) Magmatic foliations of Lower Wide Canyon (3762000-3758000 N). C) Magmatic foliations of Middle Wide Canyon (3765000-3762000N). D) Planes of late stage aplite dikes across the field area.

Zircon Geochronology

U-Pb zircon geochronology and trace element geochemistry on 8 samples reveals metamorphic rocks of Proterozoic age and igneous rocks of Cretaceous age. A bimodal concordant age distribution is reported between both Proterozoic and Cretaceous samples (Fig. 5), with significant geochemical variations among synchronous samples (Table 1). Weighted average ages were calculated using Isoplot® and are reported on concordant zircon grains (confirmed by Concordia and Tera-Wasserburg diagrams) yielding age ranges of 1.7/1.4 Ga and 88-84/76-72 Ma for Proterozoic and Cretaceous samples respectively (Ludwig, 1991).

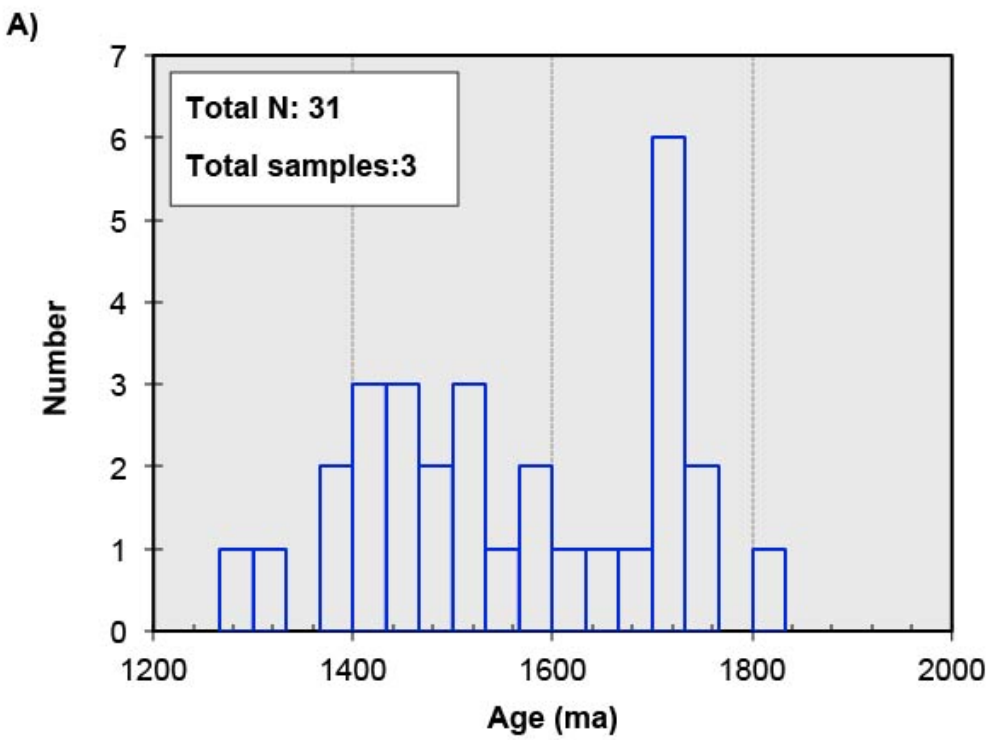

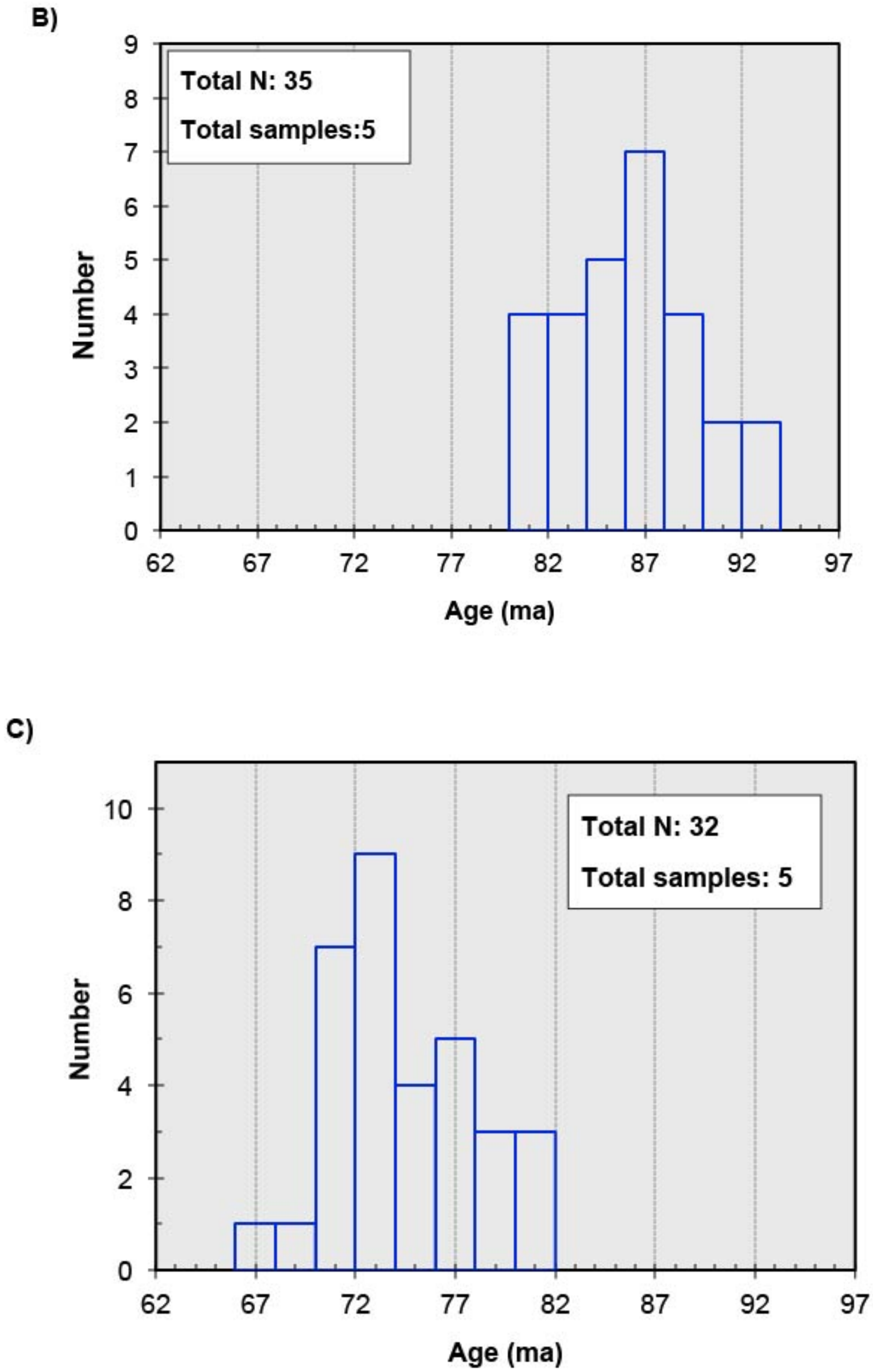

Figure 5. Probablitity density function plots for Wide Canyon samples. A) Strongly bimodal Proterozoic metaigneous and metasedimentary samples and B) Zircon cores of igneous rocks. C) Zircon rims of igneous rocks.

Table 1
U/Pb Geochron analyses via SHRIMP-RG.

Sample #	Location (UTM 11N)	Location (NAD1983)	Assemblage	Rock Type	N	Age
BPF-16-40.1 c	[0555662, 3768434]	[-116.3969, 34.0551]	Sheeted complex	metagranite	4	1519 ± 220
BPF-16-40.1 r	[0555662, 3768434]	[-116.3969, 34.0551]	Sheeted complex	metagranite	5	1390 ± 87
BPF-16-49.1	[0555974, 3763539]	[-116.3938, 34.010]	Middle Wide Canyon	garnet mylonite	8	1521 ± 60
BPF-16-49.2 c	[0555974, 3763539]	[-116.3938, 34.010]	Middle Wide Canyon	gneiss	9	1705 ± 41
BPF-16-49.2r	[0555974, 3763539]	[-116.3938, 34.010]	Middle Wide Canyon	gneiss	5	1408 ± 60
BPF-16-49.4	[0555974, 3763539]	[-116.3938, 34.010]	Middle Wide Canyon	granite	11	74.1 ± 1.6
BPF-16-54.1 c	[0556093, 3763087]	[-116.3925, 34.0069]	Lower Wide Canyon	monzodiorite	10	86.0 ± 1.8
BPF-16-54.1 r	[0556093, 3763087]	[-116.3925, 34.0069]	Lower Wide Canyon	monzodiorite	6	76.4 ± 3.5
BPF-16-57.1 c	[0557211, 3759597]	[-116.3807, 33.9754]	Lower Wide Canyon	granite	4	88 ± 6
BPF-16-57.1 r	[0557211, 3759597]	[-116.3807, 33.9754]	Lower Wide Canyon	granite	3	78 ± 0
BPF-16-57.2 c	[0557211, 3759597]	[-116.3807, 33.9754]	Lower Wide Canyon	gabbro	12	84 ± 3
BPF-16-57.2 r	[0557211, 3759597]	[-116.3807, 33.9754]	Lower Wide Canyon	gabbro	6	74 ± 3
BPF-16-58.1 c	[0557524, 3757825]	[-116.3774, 33.9594]	Lower Wide Canyon	granodiorite	8	88.5 ± 3.2
BPF-16-58.1 r	[0557524, 3757825]	[-116.3774, 33.9594]	Lower Wide Canyon	granodiorite	4	71.1 ± 3.7

c- zircon core analysis
r-zircon rim analysis

Zircons from three metamorphic samples analyzed via SHRIMP-RG all yield bimodal $^{207}Pb/^{206}Pb$ age distributions of 1.7 and 1.4 Ga. Sample BPF-16-40.1 is a potassium feldspar augen gneiss of the Upper Wide Canyon Assemblage. Porphyroblastic texture is defined by cm scale potassium feldspar augens supported by quartz, plagioclase, and biotite. Zircons are subhedral and slightly resorbed with well-defined oscillatory zoning in cathodoluminescence imaging (CL). Zircon cores and rims yield $^{207}Pb/^{206}Pb$ ages of 1590 ± 220 and 1390 ± 87 respectively (Fig. 6). One analyses was excluded from age calculation due to large errors. Sample BPF-16-49.1 is a garnetiferous mylonitic paragneiss of Middle Wide Canyon assemblage. Mineral assemblage of quartz, plagioclase, biotite and mm to cm scale garnet porphyroblasts. Zircons are rounded with poorly defined oscillatory zoning. Analyses yield a weighted mean average $^{207}Pb/^{206}Pb$ age of 1521 ± 60 (Fig. 6). Two samples were excluded from age calculations. Sample BPF-16-49.2 is a mylonitic paragneiss of Middle Wide Canyon assemblage with leucosomes of quartz and strongly altered euhedral plagioclase and melanosomes of amphibole, biotite, chlorite and epidote. Anhedral zircons are highly fractured and strongly resorbed with oscillatory zoning. Cores and rims yield weighted mean average $^{207}Pb/^{206}Pb$ ages of 1705 ± 41 and 1408 ± 60 respectively (Fig. 6).

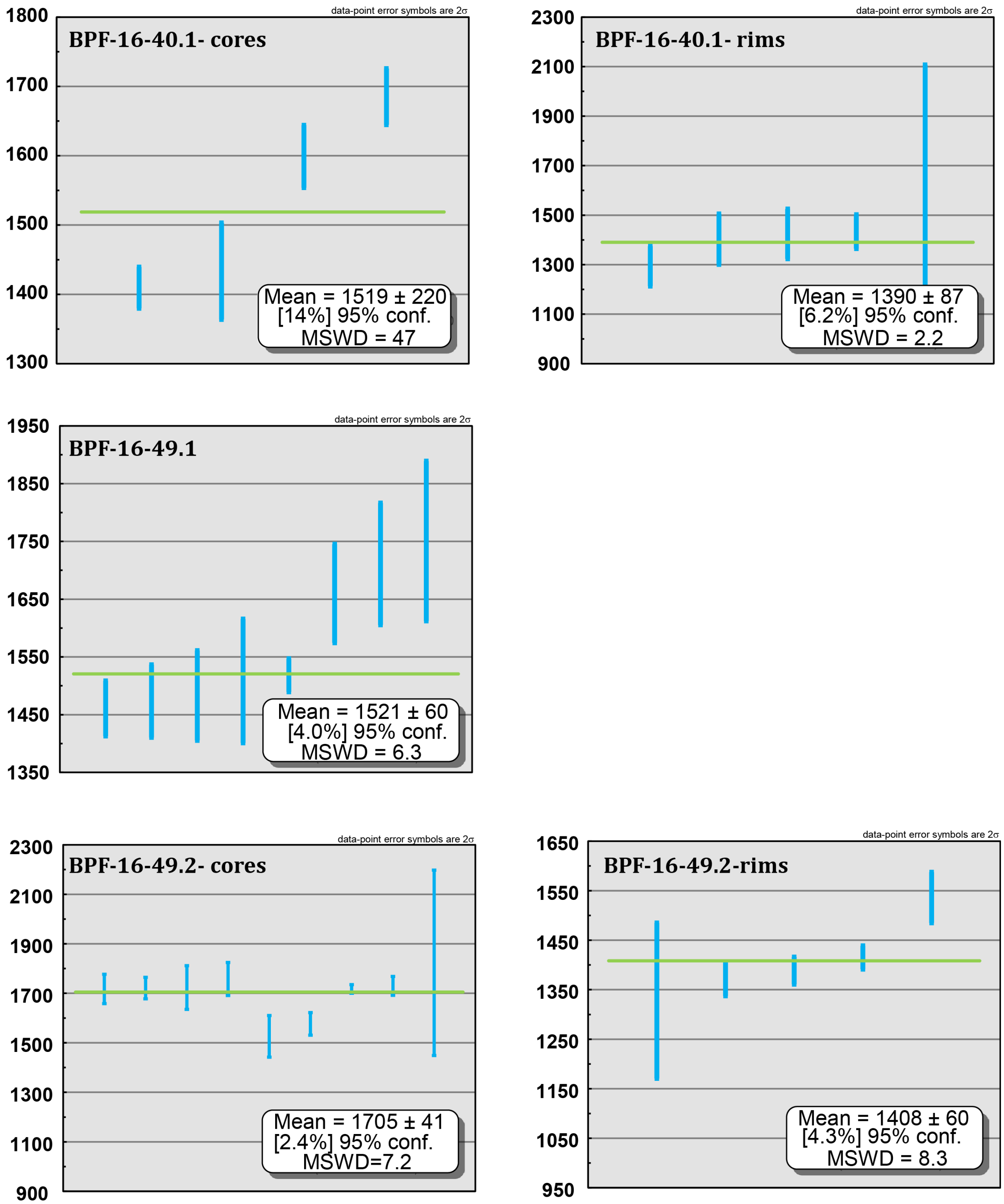

Figure 6. $^{207}Pb/^{206}Pb$ geochronology of Proterozoic metamorphic rocks of Wide Canyon. Weighted average age calculations of metamorphic rock samples of Wide Canyon yield a bimodal age population of approximately 1.7 and 1.4 Ga. Excluded ages not shown.

Five igneous samples were analyzed via SHRIMP-RG yielding a bimodal distribution of Late Cretaceous ages with no Proterozoic zircon inheritance (Fig. 7). Sample BPF-16-49.4 is a granite from the Middle Wide Canyon assemblage. Zircons are euhedral with occasional fractures and well-defined oscillatory zones in CL imaging but lacked CL bright rims observed in other igneous samples. This sample yielded a single coherent population of $^{206}Pb/^{238}U$ ages of 74.1 ± 1.6 ma with two analyses excluded from age calculation (Fig. 7). Sample BPF-16-54.1 is a monzodiorite of Middle Wide Canyon assemblage. CL analyses reveals moderate to well defined oscillatory zoning with bright cores and dark rims among euhedral to subhedral slightly fractured zircon grains. This sample yielded $^{206}Pb/^{238}U$ ages of 86 ± 1.8 and 78 ± 5.5 ma among cores and rims respectively (Fig. 7). Three samples were excluded from age calculation due to excessive error. Sample BPF-16-57.1/2 is a pair of samples of granite and an included mafic enclave of Lower Wide Canyon assemblage. Zircons are fractured with irregular and slightly resorbed grain boundaries. Zoning is irregular but shows well-defined bright rims and dark cores in CL imaging that yielded $^{206}Pb/^{238}U$ ages of 84.1 ± 3.1 and 73.9 ± 2.5 ma among cores and rims respectively with four samples excluded from age calculation (Fig. 7). Sample BPF-16-58.1 is a sheared granite of the Lower Wide Canyon assemblage. Zircon grains are euhedral with well-defined oscillatory zones consisting of bright rims and dark cores in CL, which yielded $^{206}Pb/^{238}U$ ages of 88.5 ± 3.2 and 80 ± 8.7 Ma for cores and rims respectively (Fig. 7). Twelve samples were excluded from age calculation due to large errors.

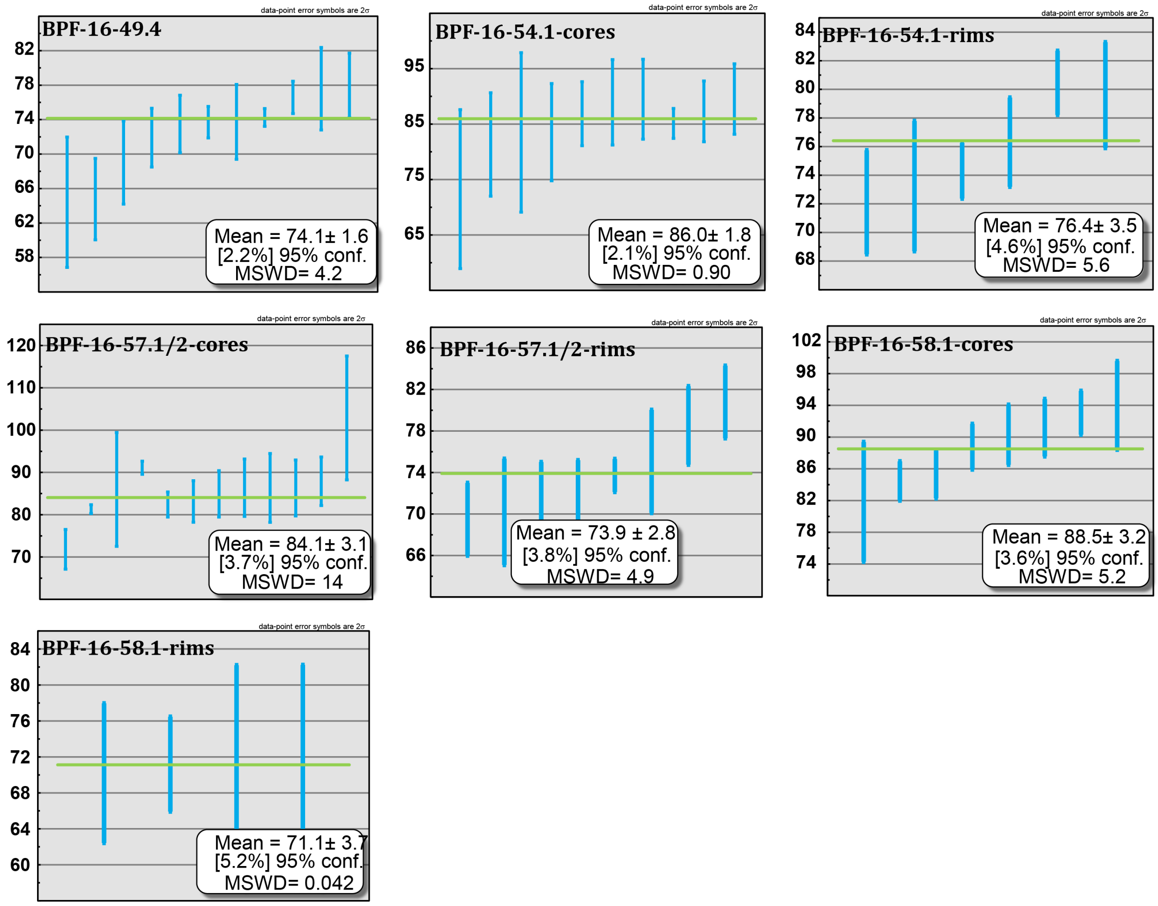

Figure 7. $^{206}Pb/^{238}U$ geochronology of Cretaceous igneous rocks of Wide Canyon. Weighted average age calculations of igneous rock samples of Wide Canyon yields a bimodal age population of approximately 88-84 Ma and 76-72 Ma. Excluded ages not shown.

CHAPTER 5

DISCUSSION

Late Cretaceous Magmatism in Wide Canyon

Field observations, petrographic analyses and zircon U-Pb geochronology reveal two phases of zircon growth in Cretaceous Wide Canyon rocks, with synkinematic shear during the Late Cretaceous from 76-72 Ma. Cretaceous geochronology samples are of wide compositional range, from gabbro to granite. Zircon geochemistry and whole rock geochemistry give some insight into whether one or both of these events were responsible for the formation of the first-order compositional variation and intrusion character observed in Wide Canyon. Zircon geochemistry shows different styles of variability in U and Th concentrations in 88-84 vs. 76-72 grains. The most significant geochemical variability is observed in magmatic zircon cores from all samples, which yield $^{238}U/^{206}Pb$ ages from 88-84 Ma. U vs Th in zircon cores exhibit orders of magnitude variability in concentrations (Fig. 8). Unlike these cores, zircon rims ($^{238}U/^{206}Pb$ age 76-72 Ma) inhabit a relatively uniform geochemical space when plotting U vs Th (ppm). These observations imply that bulk rock compositions may represent magmatism that occurred primarily at 88-84 Ma, with the second zircon growth event representing an overprint that has a more regionally coherent geochemical signature, possibly aided by the presence or circulation of fluids associated with deformation structures.

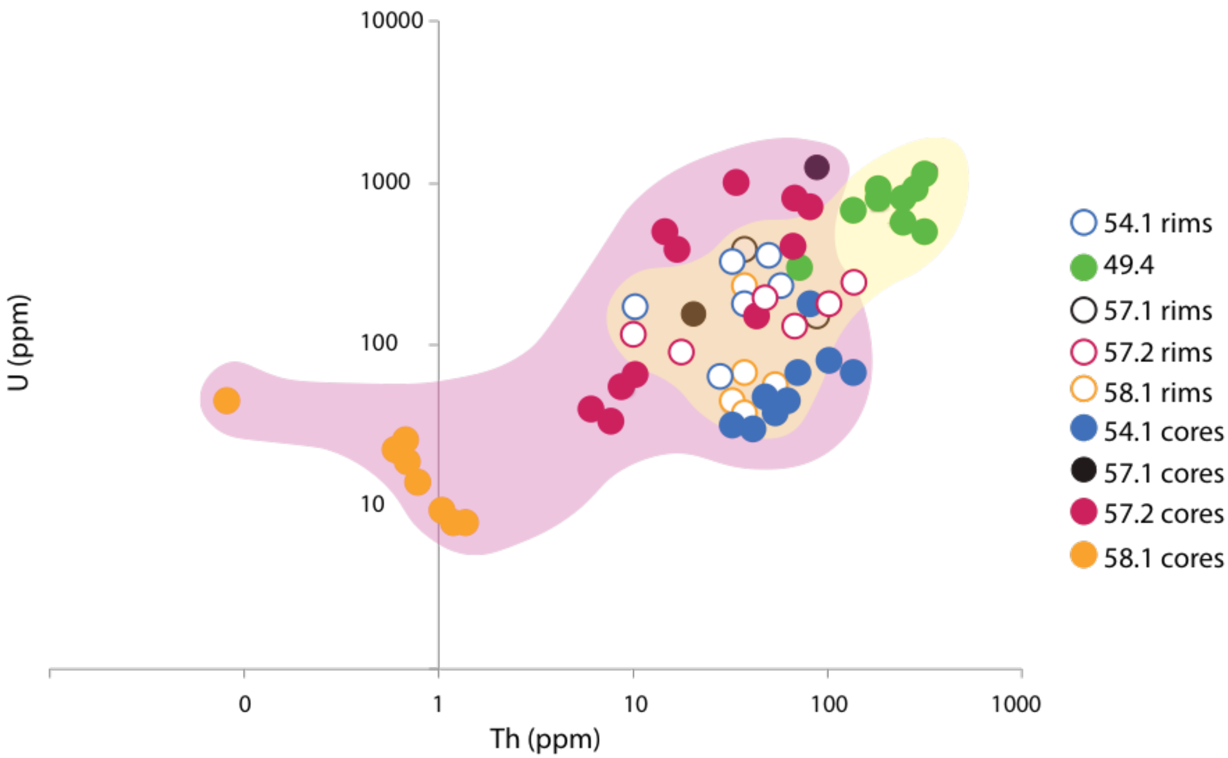

Figure 8. U vs Th of Wide Canyon igneous rocks. Logarithmic plot of U vs Th (ppm) of zircons in igneous rocks of Wide Canyon. Hollow circles represent rim analyses, filled circles represent cores. Widespread distribution of core analyses is representative of arc-derived compositions, while homogeneous rim population is a result of area wide fluid alteration at 76-72 Ma.

These are further supported through the comparison of the most mafic igneous rocks from Wide Canyon and synchronous Teutonia batholith (88-84 Ma) (Fig. 9**;** Beckerman, 1982**)**. Mafic rocks of Wide Canyon and the calc-alkaline Teutonia batholith span the same compositional range from quartz tholeiite to alkali-olivine basalt (CIPW normative) despite the lack of 76-72 Ma zircon growth in the Teutonia (Beckerman, 1982; Thompson, 1984). This suggests a similar source for mafic magmas of Wide Canyon and the Teutonia Batholith. Together with the diversity of geochemistry from 88-84 Ma zircons, the fundamental geological features of Wide Canyon are interpreted to have been constructed at 88 to 84 Ma, likely in an arc environment consanguineous with the Teutonia Batholith.

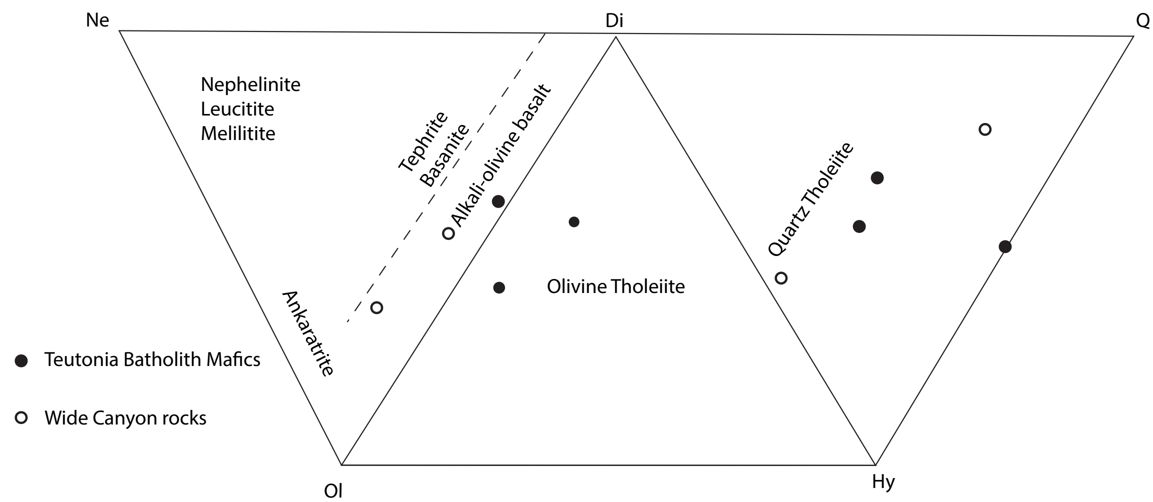

Figure 9. Compositional comparison: Teutonia Batholith and Wide Canyon. A comparison of CIPW normalizations from synchronous mafic rocks of the Teutonia batholith and Wide Canyon. Teutonia mafic rocks; black. Wide Canyon mafic rocks; white. (Beckerman*,* 1982; Thompson*,* 1984).

Hypersolidus Deformation in Wide Canyon

Northwest trending parasitic folds and a regional antiform are interpreted as synchronous with 76-72 Ma magma emplacement based on the observation of 76-72 zircon U-Pb ages of abundant of Late Cretaceous magma in parasitic fold hinges and the core of the observed regional antiform (Barraud *et al.,* 2004).

Lower portions of Wide Canyon are dominated by highly-sheared granitoids in the form of both migmatite leucosomes and plutons. High magmatic abundances coincide with high intensities of deformation, likely due to stress controlled magma emplacement and the concentration of mid-crustal shear in areas weakened by magmatism (Brown *et al.,* 1994; Sawyer *et al.,* 2001; Weinberg *et al.,* 2010). This southwest-dipping shear zone yielded diverse and abundant syn-magmatic kinematic indicators yielding top to the northeast sense of shear (Fig. 10). Observed sub and hypersolidus kinematics are interpreted in the context of U-Pb geochronology and geochemistry, implying that top to the northeast shear in the mid crust occurred between 76-72 Ma in a contractional tectonic regime. The southwest dip of the hypersolidus shear zone is the result of backthrusting in the upper plate of a larger northeast dipping thrust. The regional antiform across Wide Canyon is in the footwall of the southwest dipping backthrust. Fold axis orientations and interpreted backthrust orientation yield the same σ1 direction.

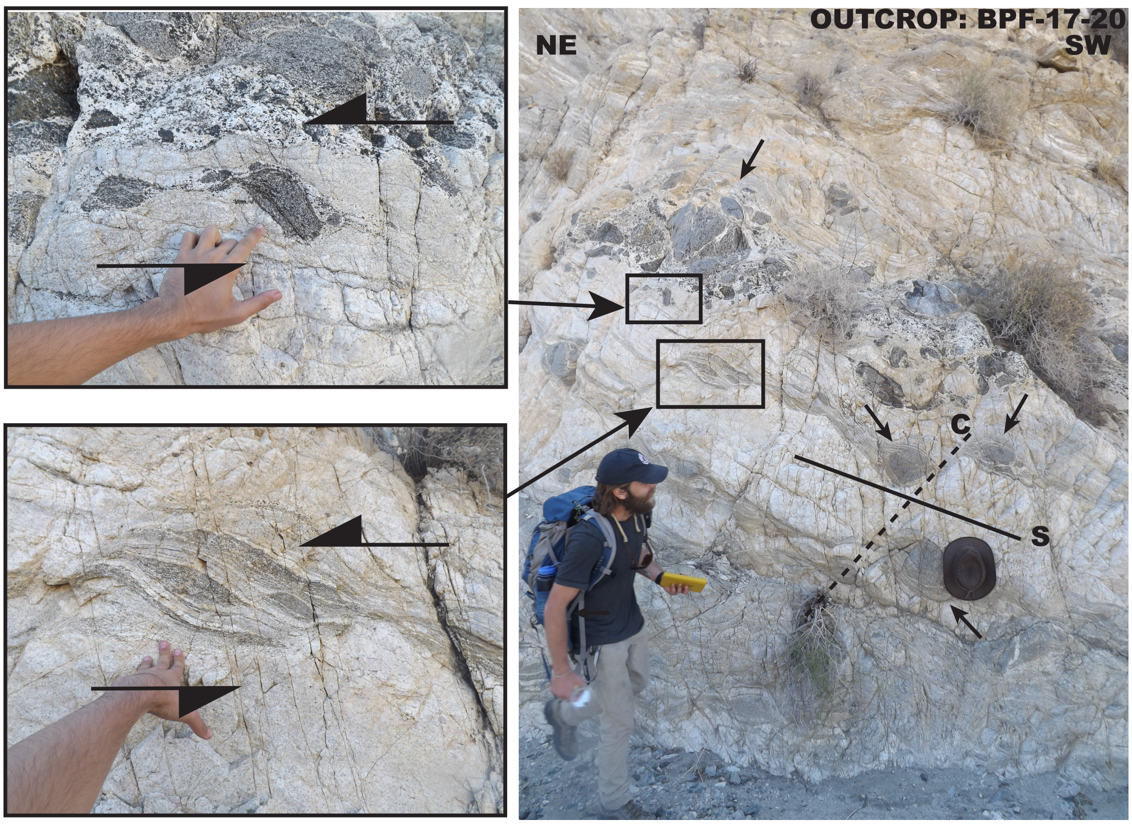

Figure 10. Hypersolidus deformation in Wide Canyon. Outcrop BPF-17-20 of Lower Wide Canyon bears an accurate representation of hypersolidus shear across the field area. An abundance of biotite/hornblende dominated mafic selvages provide top to the northeast kinematics as sigma clasts. S and C fabrics, domino structures, delta clasts and asymmetric boudins also yield top to the northeast kinematics and are abundant across the field area.

CHAPTER 6

REGIONAL IMPLICATIONS

The two zircon growth events observed in Wide Canyon are interpreted to represent two regional tectonic regimes: 1) 88-84 Ma zircon growth during the emplacement of arc magmas during the Sevier Orogeny, and 2) 76-72 Ma zircon growth during synkinematic magma emplacement and possible fluid flux accompanying the onset of Laramide flat slab subduction.

Granitoids with 88-84 Ma $^{206}Pb/^{238}U$ ages are abundant in Wide Canyon and the sheeted complex of the Little San Bernardino Mountains (Barth *et al.,* 2004; Needy *et al.,* 2009). To the north, biotite granodiorite of the Teutonia batholith from Mid Hills yields a singular rim $^{206}Pb/^{238}U$ age of 88.2 ± 1.2 Ma (Barth *et al.,* 2004). A biotite granite of the Teutonia batholith from Kessler Springs yields a singular $^{206}Pb/^{238}U$ age of 82.3 ±1.6 Ma (Fig. 11; Barth *et al.,* 2004).

Granitoid intrusions with 76-72 Ma $^{206}Pb/^{238}U$ ages are present in a broad band across the eastern and central Mojave Desert including the voluminous Cadiz Valley Batholith (Barth *et al.,* 2004; Needy *et al.,* 2009). Zircon rims on samples ranging from granite to gabbro and all zircons from a granite that intrudes the anticlinal core yield ages from 76-72 Ma. Granitic rocks of this age are present at all levels across the tilted crustal section, implying regional, high-volume magma emplacement (Barth *et al.,* 2004; Needy *et al.,* 2009; Economos *pers comm., 2018*).

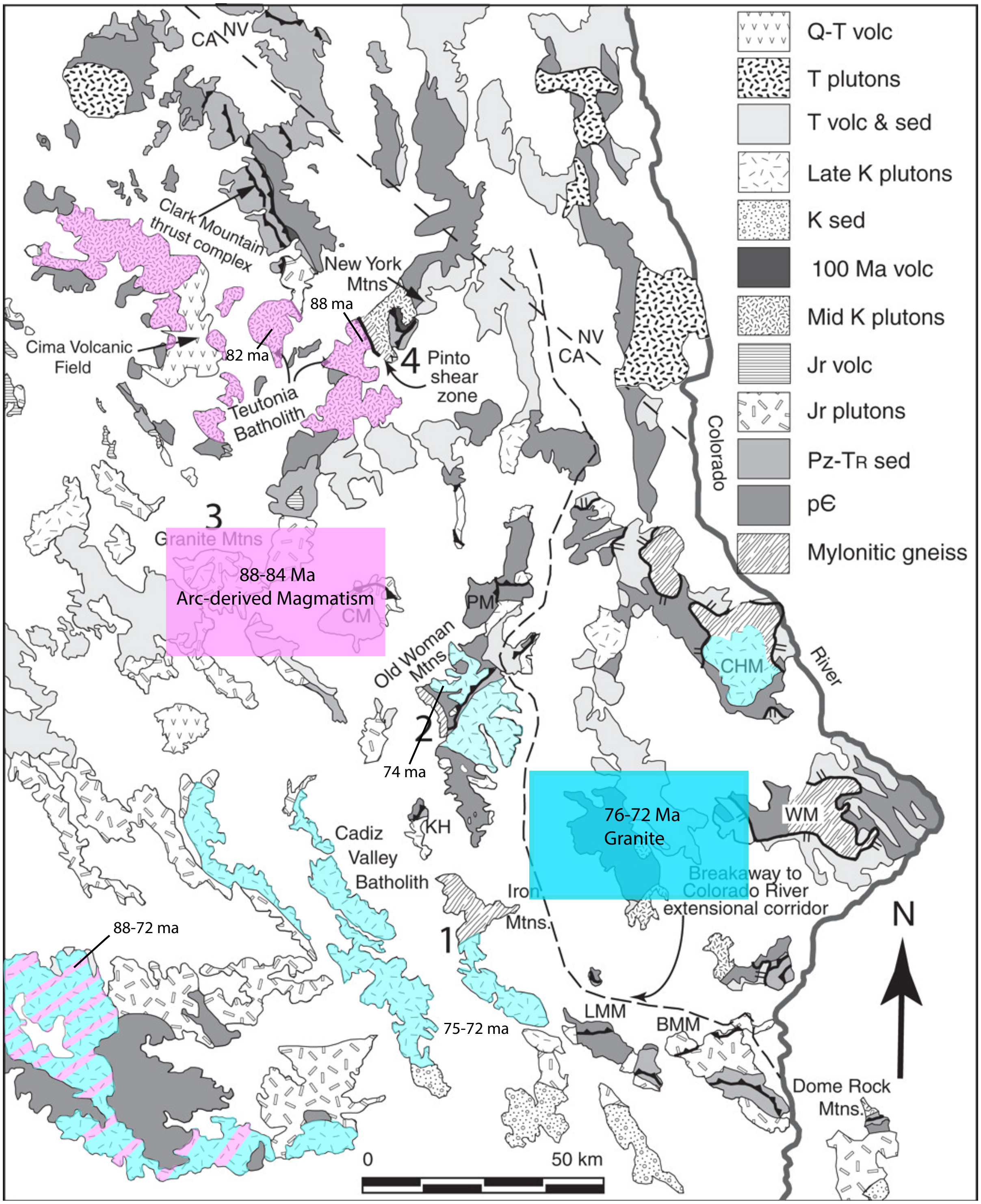

Figure 11. U-Pb age populations of the Mojave Desert region. A regional analysis of U-Pb zircon ages across the Mojave desert reveals the geometry of arc-derived magmas of the Sevier Orogeny (88-84 Ma; pink) and a narrow band of Laramide related magmas (76-72; blue). Both processes are recorded in the Little San Bernardino Mtns. (blue and pink). BM- Big Maria Mtns. CM- Coxcomb Mtns. PM- Pinto Mtns. CHM- Chemehuevi Mtns. KH-. Kilbeck Hills. WM- Whipple Mtns. LMM- Little Maria Mtns.

Rocks yielding 76-72 Ma ages in Wide Canyon are found in a mid-crustal regional top to the northeast shear zone. Observed top to the northeast kinematics on this southwest dipping structure, paired with the presence of 76-72 Ma magma in the hinges of both parasitic folds and regional NW trending antiforms appear to be the result of regional compression at 76-72 Ma. Observed NE/SW kinematic structures of the Chocolate Mountains Anticlinorium are constrained through $^{40}Ar/^{39}Ar$ dating to have occurred as a result of extension at approximately 60 Ma, during exhumation of the lower plate, not during original underthrusting of Francisican derived sediments beneath the subduction complex (Haxel, 2015; Jacobson *et al.,* 1996). We interpret observed structures and kinematic indicators in Wide Canyon to be the result of contraction on a structure that was antithetic (west-dipping) to the main thrust structures that underplated schists during the initiation of Laramide tectonics prior to the formation of the Chocolate Mountains Anticlinorium (Fig. 12).

This feature is therefore in a family of interpreted Laramide structures, including the Vincent Thrust and structures in the Orocopia Mountains. However, those structures are discrete fault zones that were reactivated by basin and range normal faulting. The shear zone in Wide Canyon appears to have Laramide-aged deformation without overprinting, likely because the zone was sealed shut by the crystallization of igneous rocks and was not a preferred fracture for re-activation. The thrust nature of this shear zone and the precise timing constrained by zircon geochronology is indicative of the crust being in a compressional environment during the widespread emplacement of 76-72 Ma granites. Our findings are in conflict with previous tectonic interpretations that 76 – 72 Ma granites were emplaced during an extensional regime at, or shortly following the onset of the Laramide Orogeny across the southern California batholith (Wells and Hoisch, 2008).

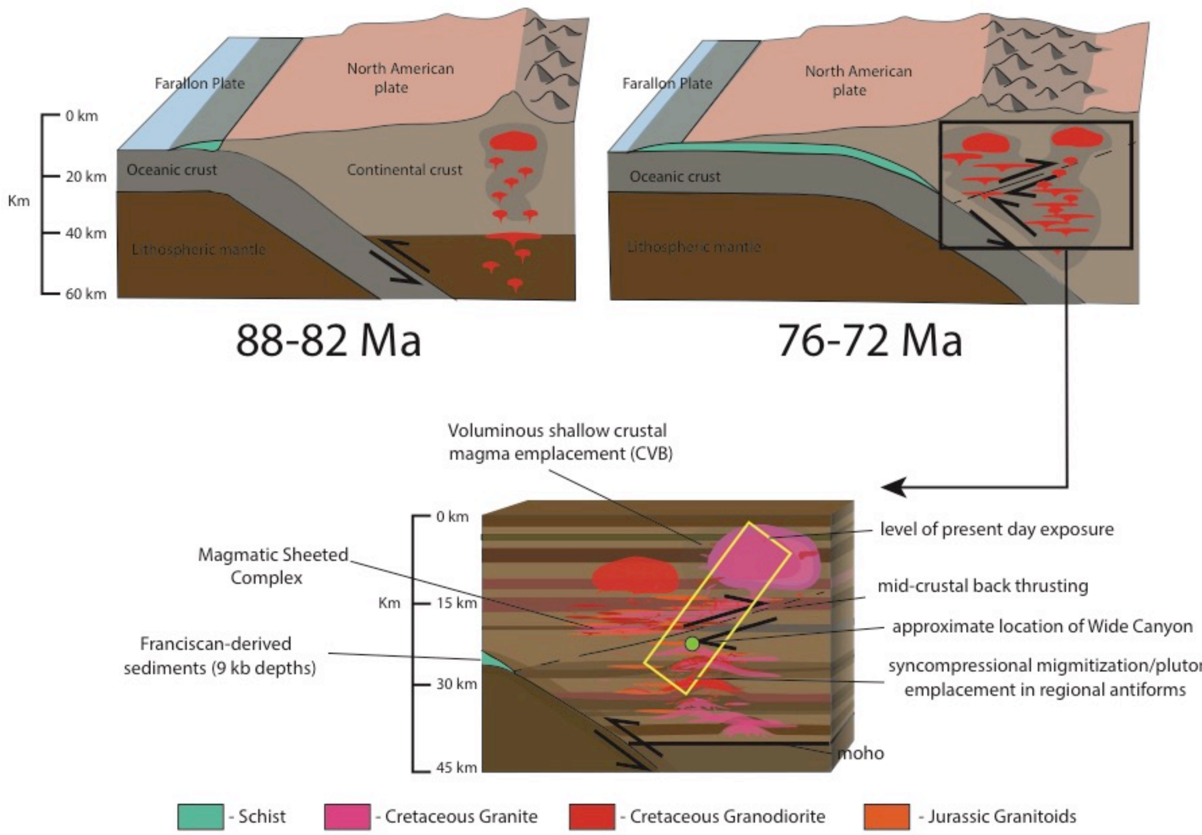

Figure 12. Synmagmatic backthrusting and compression. Andean style subduction across the Mojave portion of the Cordilleran Arc (88-82 Ma) gave way to flat slab subduction and resultant underplating of Pelona-Orocopia Schist protolithic sediments (green) and syncompressional magmatism.

CHAPTER 7

CONCLUSIONS

Wide Canyon is a 16-km-long, north/south-trending canyon in the Little San Bernardino Mountains of the eastern Transverse Ranges. The canyon preserves continuous exposure of metamorphic country rock of Proterozoic age intruded by Cretaceous granitoids in a northwest-trending regional antiform. This melt-filled northwest trending antiform is found in the footwall of a regional southwest dipping thrust. The regional antiform, parasitic folds and kinematic indicators in a regional shear zone all indicate a northeast/southwest $\sigma 1$ direction during hypersolidus conditions that can be chronologically constrained by igneous zircons.

Zircons from seven igneous rock samples yield bimodal U-Pb ages with 88-84 Ma cores and 76-72 Ma rims. One sample yielded a unimodal age of 74.1 ± 1.6 Ma. U and Th concentrations are highly variable among zircon cores, while zircon rims yield concentrations within an order of magnitude. This age distribution brackets the shift from Sevier to Laramide tectonics during the Late Cretaceous. Zircon core ages of 88-84 Ma are synchronous with rocks of the Teutonia Batholith, which is interpreted as arc-derived. Bulk rock geochemistry of mafic units in the two areas overlap. This correlation in age and chemistry, along with a good fit between whole-rock and zircon geochemical heterogeneity of 88-84 Ma cores leads to the interpretation that the major rock-forming event occurred at 88-84 Ma. The presence of more homogeneous zircon geochemistry despite the compositional range from granite to gabbro, in addition to the presence of a granite sample from a fold axis with a single age population at ~74

Ma leads to the interpretation of zircon rim ages of 76-72 Ma as recording a deformation event, the emplacement of some granites, and widespread zircon overgrowth.

Top to the northeast kinematics in the southwest dipping synmagmatic regional shear zone are interpreted as backthrusting during northwest/southeast compression with the onset of Laramide flat slab subduction. Such conclusions proclude syn-magmatic extension in the mid-crust during flat-slab subduction at the onset of the Laramide orogeny as suggested by some workers (Wells and Hoisch, 2008). Furthermore, U-Pb geochronology provides precise constraints on the timing, strain orientation and style of deformation during the Laramide Orogeny.

BIBLIOGRAPHY

Anderson, J.L., 1988, Core complexes of the Mojave-Sonoran desert: Conditions of plutonism, mylonitization, and decompression. In: Ernst, W.G. (ed) Metamorphism and Crustal Evolution of the Western United States. Englewood Cliffs, New Jersey: Prentice Hall, pp. 503 – 525.

Anderson, J.L., and Bender, E.E., 1989, Nature and origin of Proterozoic A-type magmatism in the southwestern United States of America: Lithos v. 23, p. 19 – 52.

Anderson, J.L., and Morrison, J., 1992, The Role of Anorogenic Granites in the Proterozoic Crustal Development of North America: Developments in Precambrian Geology, v. 10, p. 263-299.

Annen, C., Blundy, J.D., and Sparks, R.S.J., 2006, The genesis of intermediate and silicic magmas in deep crustal hot zones: Journal of Petrology, v. 47(3), p. 505–539.

Bachmann O., and Bergantz G., 2008, The magma reservoirs that feed supereruptions: Elements, v. 4, p. 17–21.

Barraud J., Gardien V., Allemand P., and Grandjean P., 2004, Analogue models of melt-flow networks in folding migmatites: Journal of Structural Geology, v. *26*(2), p. 307-324.

Barth, A.P., and May, D.J., 1992, Mineralogy and pressure-temperature-time path of Cretaceous granulite gneisses, southeastern San Gabriel Mountains, southern California. Journal of Metamorphic Petrology, v. 10, p. 529-544.

Barth, A.P., Wooden, J.L., Tosdal, R.M., and Morrison, J., 1995, Crustal contamination in the petrogenesis of a calc-alkaline rock series: Josephine Mountain Intrusion, California: Geological Society of America Bulletin, v. 107, p. 201-212.

Barth, A.P., Wooden, J.L., and Coleman, D.S., 2001, SHRIMP-RG U-Pb Zircon Geochronology of Mesoproterozoic Metamorphism and Plutonism in the southwesternmost United States: Geology, v. 109 (3), p. 319-327.

Barth, A.P., Wooden, J.L., Jacobsen, C.E., and Probst, K., 2004, U-Pb geochronology and geochemistry of the McCoy Mountains formation, southeastern Calfiornia: A Cretaceous retroarc foreland basin: Geological Society of America Bulletin, v. 116, p. 142-153.

Barth, A.P., and Wooden, J.L., 2006, Timing of magmatism following initial convergence at a passive margin, southwestern U.S. Cordillera, and ages of lower crustal magma sources: Journal of Geology, v. 114, p. 231–245.

Barth, A.P., Wooden, J.L., Coleman, D.S., and Vogel, M.B., 2009, Assembling and Disassembling California: A Zircon and Monazite Geochronologic Framework for Proterozoic Crustal Evolution in Southern California: Journal of Geology, v. 117, p. 221 – 239.

Barth A.P., and Wooden, J.L, 2010, Coupled elemental and isotopic analyses of polygenetic zircons from granitic rocks by ion microprobe, with implications for melt evolution and the sources of granitic magmas: Chemical Geology, v. 277(1), p. 149-159.

Barth, A.P., Wooden, J.L., Jacobson, C.E., and Economos, R.C., 2013, Detrital zircon as a proxy for tracking the magmatic arc system: the California arc example: Geology, v. 41 (2), p. 223–226.

Bateman, P. C., and Chappell, B. W., 1979, Crystallization, fractionation and solidification of the Tuolumne intrusive series, Yosemite National Park, California: Geological Society of America Bulletin, V. 90, p. 465-82.

Bateman, P.C., 1992, Plutonism in the central part of the Sierra Nevada Batholith, California: U.S. Geological Survey Professional Paper, v. 1483, p. 186.

Black, L.P., Kamo, S.L., Allen, C.M., Davis, D.W., Aleinikoff, J.N., Valley, J.W., Mundil, R., Campbell, I.H., Korsch, R.J., Williams, I.S., and Foudoulis, C., 2004, Improved Pb-206/U-218 microprobe geochronology by the monitoring of a trace-elementrelated matrix effect; SHRIMP, ID-TIMS, ELA-ICP-MS and oxygen isotope documentation for a series of zircon standards: Chemical Geology v. 205, p. 115–140.

Boehnke, P., Watson, B., Trail, D., Harrison, M., and Schmitt, A., 2013, Zircon Saturation Re-revisited: Chemical Geology, v. 351 p. 324-34, doi: 10.1016/j.chemgeo.2013.05.028.

Burns, D.H., de Silva, S.L., Tepley III, F., Schmitt, A.K., and Loewen, M.W., 2015, Recording the transition from flare-up to steady-state arc magmatism at the Purico Chascon volcanic complex, northern Chile: Earth Planetary Science Letters. v. 422, p. 75–86.

Brophy, J. G., 1991, Composition gaps, critical crystallinity, and fractional crystallisation inorogenic (calc-alkaline) magmatic systems: Contributions to Mineralogy and Petrology., v. 109, p.173–182.

Calzia, J.P., 1982, Geology of granodiorite in the Coxcomb Mountains, southeastern California. In: Frost, E.G. & Martin, D.L. (eds) Mesozoic-Cenozoic tectonic evolution of the Colorado River region, California: Cordilleran Publishers, pp. 173 – 180.

Carter, J.N., Luyendyk, B.P., and Terres, R.P., 1987, Neogene clockwise tectonic rotation of the eastern Transverse Ranges, California, suggested by paleomagnetic vectors: Geological Society of America Bulletin, v. 98 (2), p. 199-206.

Chmieloswki, J., Zandt, G., and Haberland, C., 1999, The central Andean Altiplano-Puna magma body: Geophysical Research Letters, v. 26, p. 783-786.

Clark, G.L., White, R.W., Lui, S., Fitzherbert, J.A., and Pearson, N.J., 2007, Contrasting behavior of rare earth and major elements during partial melting in granulite facies migmatites, Wuluma Hills, Arunta Block, central Australia: Journal of Metamorphic Geology, v. 25, p. 1-18. doi:10 1111/j.1525-1314.2006.00673.

Coleman, D.S., Gray, W., Glazner, A.F., 2004, Rethinking the emplacement and evolution of zoned plutons: geochronologic evidence for incremental assembly of the Tuolumne Intrusive Suite, California: Geology, v. 32(5), p. 433–436.

Copeland, P., Currie, C.A., Lawton, T. F., Murphy, M.A., 2017, Location, location, location: The variable lifespan of the Laramide orogeny: Geology, v. 45(3), p. 223-224.

Coney, P.J., and Reynolds, S.J., 1977, Cordilleran Benioff zones: Nature, v. 270, p. 403-406.

Daly, R.A., 1925, The geology of Ascension Island: American Academy of Arts and Sciences Proceedings, v. 60, p. 1–80.

de Silva, S.L., 1989, Altiplano-puna volcanic complex of the central Andes: Geology, v. 17, p. 1102-1106.

de Silva, S.L., Zandt, G., Trumbull, R., Viramonte, J.G., Salas, G., and Jimenez, N., 2006, Large ignimbrite eruptions and volcano-tectonic depressions in the Central Andes: a thermomechanical perspective: Geological Society of London Special Publications, v. 269, p. 47-63.

de Silva, S.L. and Gosnold, W.D. , 2007, Episodic construction of batholiths: insights from the spatiotemporal development of an ignimbrite flare-up: Journal of Volcanology and Geothermal Research, v. 167, p. 320-335.

DeBari, S.M., Sleep, N.H., 1991, High-Mg, low-Al bulk composition of the Talkeeta island arc, Alaska: implications for primary magmas and the nature of arc Crust: Geological Society of America Bulletin, v. 103, p. 37-47.

DeCelles, P., 2004, Late Jurassic to Eocene evolution of the Cordilleran thrust belt and foreland basin system, western USA: American Journal of Science, v. 304, p. 105.

Depaolo, D.J., 1981, Trace element and isotopic effects of combined wallrock assimilation and fractional crystallization: Earth and Planetary Science Letters, v. 53 (2), p. 189-202.

Dickinson, W.R., and Snyder, W.S., 1978, Plate Tectonics of the Laramide Orogeny, Laramide Folding Associated with Basement Block Faulting in the Western United States, Vincent Matthews, III.

Ducea, M., 2001, The California arc: Thick granitic batholiths, eclogitic residues, lithospheric-scale thrusting, and magmatic flare-ups: GSA Today, v. 11(11), p. 4-10.

Ducea, M.N., and Barton, M.D., 2007, Igniting flare- up events in Cordilleran arcs: Geology, v. 35, p. 1047–1050.

Dufek, J., and Bachmann, O., 2010, Quantum magmatism: magmatic compositional gaps generated by melt-crystal dynamics: Geology*, v.* 38, p. 687-690.

England, P., Wilkins, C., 2004, A simple analytical approximation to the temperature structure in subduction zones: Geophysical Journal International, v. 159, p. 1138–1154.

Glazner, A.F., Bartley, J.M., Coleman, D.S., Gray, W., Taylor, Z.T., 2004, Are plutons assembled over millions of years by amalgamation from small magma chambers?: GSA Today, v. 14 (4/5), p. 4–11.

Grove, Marty, et al., 2003, Temporal and spatial trends of Late Cretaceous-early Tertiary underplating of Pelona and related beneath southern California and southwestern Arizona: Tectonic evolution of northwestern Mexico and the southwestern USA*,* p. 374 381.

Grove, T. L. and Donnelly-Nolan, J. M., 1986, The evolution of young silicic lavas at Medicine Lake Volcano, California: Implications for the origin of compositional gaps in calc-alkaline series lavas: Contributions to Mineralogy and Petrology, v. 92, p. 281-302.

Haxel, G.B., Jacobson, C.E., and Wittke, J.H., 2015, Mantle peridotite in newly discovered far-inland subduction complex, southwest Arizona: Initial report: International Geology Review, v. 57, p. 871–892, doi:10.1080/00206814.2014.928916.

Hildreth, W., and Moorbath, S., 1988, Crustal contribution to arc magmatism in the Andes of Central Chile: Contributions to mineralogy and petrology, v. 98, p. 455–489.

Holk, Gregory J., et al., 2017, A two-stage fluid history for the Orocopia Schist and associated rocks related to flat subduction and exhumation, southeastern California: International Geology Review, v. 59.5-6, p. 639-663.

Hoskin, P., 2003, The Composition of Zircon and Igneous and Metamorphic Petrogenesis: Reviews in Mineralogy and Geochemistry, v. *53*(1), p. 27-62.

Howard, K.A., and John, B. E., 1984, Geologic map of Sheep Hole-Cadiz WIderness Study Area (CDCA-305), San Bernardino, California; USGS 1615A.

Howard, K.A., 2002, Geologic Map of the Sheep Hole Mountains 30'x 60' Quadrangle, San Bernardino and Riverside Counties, CA: USGS MF- 2344.

Humphreys, E.D., 1995, Post-Laramide removal of the Farallon slab, western United States: Geology, v. 23 (11), p. 987-990.

Ianno, Adam J., 2015, Studies of the Late Cretaceous Magmatic Crustal Column at Joshua Tree National Park, California: University of Southern California, Doctor of Philosophy Dissertation, 300 pp.

Isacks, B.L., 1988, Uplift of the Central Andean Plateau and bending of the Bolivian orocline: Journal of Geophysical Research, v. 93 p. 3211-3231.

Jacobson, C., 1983, Structural geology of the Pelona Schist and Vincent thrust, San Gabriel Mountains, California. Geological Society of America Bulletin, v. 94(6), p. 753-767.

Jacobson, C.E., 1995, Qualitative thermobarometry of inverted metamorphism in the Pelona and Rand Schists, southern California, using calciferous amphibole in mafic schist: Journal of Metamorphic Geology, v. 13(1), p. 79-92.

Jacobson, C. E., and Dawson, M. R., 1995, Structural and metamorphic evolution of the Orocopia Schist and related rocks, southern California: Evidence for late movement on the Orocopia fault, Tectonics, 14(4), p. 933–944, doi:10.1029/95TC01446.

Jacobson, C. E., Oyarzabal, Felix R., and Haxel, Gordon B. (1996). Subduction and exhumation of the Pelona-Orocopia-Rand schists, southern California. Geology, v. 24(6), p. 547.

Jacobson, C., Barth, A., and Grove, M., 2000, Late Cretaceous protolith age and provenance of the Pelona and Orocopia Schists, southern California: Implications for evolution of the Cordilleran margin. Geology, v. 28(3).

Jagoutz, O., Muntener, O., Ulmer, P., Pettke, T., Burg, J - P., Dawood, H., and Hussain, S., 2007, Petrology and mineral chemistry of lower crustal intrusions: the Chilas Complex, Kohistan (NW Pakistan): Journal of Petrology, v. 48, p. 1895–1953.

Kapp, J., Miller, C., and Miller, J., 2002, Ireteba Pluton, Eldorado Mountains, Nevada: Late, Deep-Source, Peraluminous Magmatism in the Cordilleran Interior: The Journal of Geology, v. 110(6), p. 649-669, doi:10.1086/342864.

Kay, S. M., Maksaev, V., Mpodozis, C., Moscoso, R., and Nasi, C., 1987, Probing the evolving Andean lithosphere; Mid-late Tertiary magmatism in Chile (29°-30.5°S) over the zone of subhorizontal subduction: Journal of Geophysical Research, v. 92, p. 6173-6189.

Kay, S. M., and 5 others, 1988, Tertiary Andean magmatism in Argentina and Chile between 28-33°S; Correlation of magmatic chemistry with a changing Benioff zone: Journal of South American Earth Sciences, v. 1, p. 21-38.

Kay, S. Mahlburg, Mpodozis, C.. Ramos. V.A. and Munizaga, F., 1991. Magma source regions for mid to late Tertiary volcanic rocks and erupted over a shallowing subduction zone and through a thickening crust in the main Andean Cordillera (28-33"s). In: R.S. Harmon and C.W. Rapela (Editors), Andean Magmatism and its Tectonic Setting. Geological Society of America Special Papers v. 265, p. 113-137.

Kay, R.W., and Mahlburg Kay, S., 1993, Delamination and delamination magmatism: Tectonophysics, v. 219, p. 177–189.

Kistler, R.W., and Champion, D.E., 2001, Rb-Sr whole-rock and mineral ages, K-Ar, $^{40}Ar/^{39}Ar$ and U-Pb mineral ages, and strontium, lead, neodymium and oxygen isotopic compositions for granitic rocks fromt eh Salinia composite terrane, California: U.S. Geological Survey Open File Report 01-453, p. 84.

Kistler, R.W., and Ross, D., 1990, A strontium isotopic study of plutons and associated rocks of the southern Sierra Nevada and vicinity, California: Dept. of the Interior, U.S. Geological Survey.

Lackey, J., Valley, J., Chen, J., and Stockli, D, 2008, Dynamic magma systems, crustal recycling and alteration in the central Sierra Nevada Batholith: the Oxygen Isotope Record: Journal of Petrology, v. 49 (7), p. 1397-1426.

Langenheim, V. E., and R. E. Powell, 2009. Basin geometry and cumulative offsets in the Eastern Transverse Ranges, southern California: Implications for transrotational deformation along the San Andreas fault system: Geosphere, v. 5**,** p. 1-22.

Leidig, M., and Zandt, G., 2003, Modeling of highly anisotropic crust and application to the Altiplano-Puna volcanic complex of the central Andes: Journal of Geophysical Research., v. 108, p. 2014.

Liu, L.,Gurnis, M., Seton, M., Saleeby, J., Müller, R. D., and Jackson, J. M, 2010, The role of oceanic plateau subduction in the laramide orogeny: Nature Geoscience*, v. 3*(5), p. 353-357, doi:http://dx.doi.org/10.1038/ngeo829.

Livaccari, R., 1991, Role of crustal thickening and extensional collapse in the tectonic evolution of the Sevier-Laramide orogeny, western United States. Geology, v. 19(11), p. 1104.

Livaccari, R.F., Burke, K., and Şengör, A.M.C., 1981, Was the Laramide orogeny related to subduction of an oceanic plateau?: *Nature*, v. 289 pp. 276-278 doi:10.1038/289276a0.

Ludwig, K., 1991, ISOPLOT: a plotting and regression program for radiogenic-isotope data (rev): Denver, Colo.: U.S. Geological Survey.

Mayo, D.P., Anderson, J.L., and Wooden, J.L., 1998, Isotopic constraints on the petrogenesis of Jurassic plutons, southeastern California: International Geology Review, v. 40, p. 421-442.

McKenzie N.R., Horton B.K., Loomis S.E., Stockli D.F, Planavsky N.J., and Lee C.A., 2016, Continental arc volcanism as the principal driver of icehouse-greenhouse variability: Science, v. 352, p. 444-447.

Meade, F.C., Troll, V.R., Ellam, R.M., Freda, C., Font, L., Donaldson, C.H., and Klonowska, I., 2014, Bimodal magmatism produced by progressively inhibited crustal assimilation: Nature Communications, v. *5*, p. 4199.

Melekhova, E., Annen, C., and Blundy, J., 2013, Compositional gaps in igneous rock suites controlled by magma system heat and water content: Nature Geoscience, v. 6, p. 385-390.

Miller, C. F., Meschter McDowell, S., Mapes, R.W., (2003). Hot and cold granites? Implications of zircon saturation temperatures and preservation of inheritance: Geology, v.31(6), p. 529-532.

Miller, J.S., Glazner, A.F., and Crowe, D.E., 1996, Muscovite-garnet granites in the Mojave Desert: Relation to crustal structure of the Cretaceous arc: Geology, v. 24, p. 335-338.

Miller, J.S., Matzel, J.P., Miller, C.F., Burgess, S.D., and Miller, R.B., 2007, Zircon growth and recycling during the assembly of large, composite arc plutons: Journal of Volcanology and Geothermal Research v. 167, 282–299.

Musumeci, Mazzarini, Corti, Barsella, and Montanari., 2005, Magma emplacement in a thrust ramp anticline: The Gavorrano Granite (northern Apennines, Italy). Tectonics, v. 24(6).

Needy, S.K., Anderson, J.L., Wooden, J.L., Barth, A.P., Paterson, S.R., Memeti, V., and Pignotta, G.S., 2009, Mesozoic magmatism in an upper to middle-crustal section through the Cordilleran continental margin arc, eastern Transverse Ranges, California, *in* Miller, R.B., and Smoke, A.W., eds., Crustal cross sections from the western North America Cordillera and else- where: Implications for tectonic and petrologic processes: Geological Society of America Special, v. 456, 187–218.

Paterson, S.R., Okaya, D., Memeti, V., Economos, R., and Miller, R.B., 2011, Magma addition and flux calculations of incrementally constructed magma chambers in continental margin arcs: combined field, geochronologic, and thermal modeling studies: Geosphere, v. 7, p. 1439–1468.

Pickett, D. A., and Saleeby, J.B., 1993, Thermobarometric constraints on the depth of exposure and conditions of plutonism and metamorphism at deep levels of the Sierra Nevada Batholith, Tehachapi Mountains, California: J. Geophys. Res., v. 98(B1), p. 609–629, doi:10.1029/92JB01889.

Powell, R.E., 1981, Geology of the crystalline basement complex, eastern Transverse Ranges, southern California [Ph.D. dissertation]: Pasadena, California Institute of Technology, 441 p.

Powell, R.E., Weldon, R., and Matti, J., 1993, The San Andreas fault system: displacement, palinspastic reconstruction, and geologic evolution: Boulder, Colo.: Geological Society of America.

Ricketts, et al., 2011, Episodic Growth of the Chocolate Mountains Anticlinorium Recorded By the Neogene Bear Canyon Conglomerate, Southeastern California, U.S.A. Journal of Sedimentary Research, v. 81(12), p.859–873.

Ridolfi, F., Renzulli, A., and Puerini, M., 2010, Stability and chemical equilibrium of amphibole in calc-alkaline magmas: An overview, new thermobarometric formulations and application to subduction-related volcanoes: Contributions to Mineralogy and Petrology, v. 160(1), p. 45-66.

Salleby, J., 2003, Segmentation of the Laramide Slab-Evidence from the southern Sierra Nevada region: Geological Society of America Bulletin, v. 115, p. 655-668, doi:10.1130/0016-7606(2003)115<0655:SOTLSF>2.0.CO;2.

Sawyer, E., 2004, Melt segregation in the continental crust: Geology, v. 22(11), p. 1019-1022. doi:10.1130/0091-7613(1994)0222.3.CO;2

Schmidt, Max W., 1992, Amphibole composition in tonalite as a function of pressure:an experimental calibration of the Al-in-hornblende barometer: Contributions to Mineralogy and Petrology, v. 110, p. 304-310.

Sharry, J., 1981, The geology of the western Tehachapi Mountains, California [Ph.D thesis]: Cambridge: Massachusetts Institute of Technology, 215 p., 3 pls.

Spera F.J., and Bohrson, W., 2001, Energy-constrained open-system magmatic processes I: General model and energy constrained assimilation-fractional crystallization (EC-AFC) formulation: Journal of Petrology, v. 42, p. 999–1118.

Suneson, N., and Lucchitta, I., 1983, Origin of bimodal volcanism, southern Basin and Range province, west-central Arizona: Bulletin of the Geological Society of America, v. 94(8), p. 1005-1019.

Tosdal, R.M., Haxel, G.B., and Wright, J.E.,1989, Jurassic geology of the Sonoran Desert region, southern Arizona, southeast California, and northernmost Sonora: Construction of a continental-margin magmatic arc. In: Jenny, J.P. & Reynolds, S.J. (eds) Geologic evolution of Arizona: Arizona Geological Society Digest, v. 17. Tucson, Arizona: Arizona Geological Society.

Voshage, H., Hofmann, A. W., Mazzucchelli, M., Rivalenti, G., Sinigoi, S., Raczek, I. and Demarchi, G., 1990, Isotopic evidence from the Ivrea Zone for a hybrid lower crust formed by magmatic underplating: Nature, v. 347, p. 731-736.

Walker, B.A., Grunder, A.L., and Wooden, J.L., 2010, Organization and thermal maturation of long-lived arc systems: Evidence from zircons at the Aucanquilcha volcanic cluster, northern Chile: Geology, v. 38, p. 1007–1010,

Ward K.M., Zandt G., Beck S.L., Christensen, D.H., and McFarlin H., 2014 Seismic imaging of the magmatic underpinnings beneath the Altiplano-Puna volcanic complex from the joint inversion of surface wave dispersion and receiver functions: Earth and Planetary Science Letters, v. 404, p. 43-53

Watson, E.B., Harrison, T.M., 1983, Zircon saturation revisited: temperature and composition effects in a variety of crustal magma types: Earth and Planetary Science Letters, v. 64, p. 295–304.

Weinberg, R. and Regenauer-Lieb, K., 2010, Ductile fractures and magma migration from source: Geology, v. 38 (4), p. 363.

Wells, M.L., Hoisch, T.D., 2008, The role of mantle delamination in widespread Late Cretaceous extension and magmatism in the Cordilleran orogen, western United States: Geological Society of America Bulletin, v. 120, p. 515–530, doi:10.1130/B26006.1.

Wiedenbeck, M., Hanchar, J.M., Peck, W.H., Sylvester, P., Valley, J., Whitehouse, M., Kronz, A., Morishita, Y., and Nasdala, L., 2004, Further characterisation of the 91500 zircon crystal: Geostandards and Geoanalytical Research, v. 28 (1), p. 9–39.

Wiegand, B.A., Barth, A.P., Wooden, J.L., Palmer, E.F., Brown, K.L., and Needy, S.L., 2007, Sr and Nd isotopic evolution in Late Cretaceous lower to upper crustal granitic rocks from the Transverse Ranges, southern California: Geological Society of America Abstracts with programs, v. 39(6), p. 407.

Wright, J.E., Howard, K.A., and Anderson, J.L., 1987, Isotopic systematics of zircons from Late Cretaceous intrusive rocks, southeastern California: Implications for a vertically stratified crustal column: Geological Society of America Abstracts with Programs, v.19, p. 898.

Zandt, G., Leidig, M., Chmielowski, J., Baumont, D., and Yuan, X., 2003, Seismic detection and characterization of the Altiplano-Puna magma body, central Andes: Pure and Applied Geophysics, v. 160, p. 789–807.